

Published in final edited form as:

Cell. 2005 October 21; 123(2): 219–231. doi:10.1016/j.cell.2005.08.036.

Genome-Wide Dynamics of Htz1, a Histone H2A Variant that Poises Repressed/Basal Promoters for Activation through Histone Loss

Haiying Zhang^{1,2}, Douglas N. Roberts^{1,2}, and Bradley R. Cairns^{1,2,*}

¹Howard Hughes Medical Institute, Department of Oncological Sciences University of Utah School of Medicine Salt Lake City, Utah 84112

²Huntsman Cancer Institute Department of Oncological Sciences University of Utah School of Medicine Salt Lake City, Utah 84112

Summary

Histone variants help specialize chromatin regions; however, their impact on transcriptional regulation is largely unknown. Here, we determined the genome-wide localization and dynamics of Htz1, the yeast histone H2A variant. Htz1 localizes to hundreds of repressed/basal Pol II promoters and prefers TATA-less promoters. Specific Htz1 deposition requires the SWR1 complex, which largely colocalizes with Htz1. Htz1 occupancy correlates with particular histone modifications, and Htz1 deposition is partially reliant on Gcn5 (a histone acetyltransferase) and Bdf1, an SWR1 complex member that binds acetylated histones. Changes in growth conditions cause a striking redistribution of Htz1 from activated to repressed/basal promoters. Furthermore, Htz1 promotes full gene activation but does not generally impact repression. Importantly, Htz1 releases from purified chromatin *in vitro* under conditions where H2A and H3 remain associated. We suggest that Htz1-bearing nucleosomes are deposited at repressed/basal promoters but facilitate activation through their susceptibility to loss, thereby helping to expose promoter DNA.

Introduction

Eukaryotic genomes are partitioned into chromatin regions of varying composition, character, and length. Though diverse in composition, there are themes to the construction of all chromatin regions. First, chromatin can bear nucleosomes formed from the four canonical histones (H2A, H2B, H3, and H4,) or nucleosomes bearing histone variants that help specialize chromatin regions (Henikoff et al., 2000; Henikoff et al., 2004; Mizuguchi et al., 2004; Smith, 2002). Whereas canonical nucleosomes are deposited during DNA replication, certain histone variants can be deposited actively in a replication-independent manner, as has been demonstrated for histone H3.3 (Ahmad and Henikoff, 2002). Second, covalent modifications (such as acetylation or methylation) are directed to nucleosomes in particular regions, which then attract additional proteins that further influence the composition and active state of the gene or region (Jenuwein and Allis, 2001). Third, nucleosomes are mobilized by complexes termed Remodelers to assume their correct positions on the DNA, which can either facilitate or impede processes such as transcription (Owen-Hughes, 2003). The order and relative importance of these three processes varies at individual loci and is guided (in part) by site-specific DNA binding proteins,

which can recruit chromatin restructuring, modifying, and remodeling factors. Together, these factors regulate the dynamic properties of chromatin.

A central question in the field of chromatin regulation is how histone variants regulate transcription (Kamakaka and Biggins, 2005). Our studies focus on Htz1, the sole histone H2A variant in the budding yeast *S. cerevisiae* and an ortholog of mammalian H2A.Z (Jackson et al., 1996). At least three features of H2A.Z/Htz1 distinguish it from H2A: (1) a unique C-terminal tail important for specifying H2A.Z/Htz1 deposition (Adam et al., 2001), (2) an extended surface charge patch (α C helix) which may help regulate chromatin compaction (Fan et al., 2004), and (3) a small internal loop that helps ensure that nucleosomes contain either two H2A.Z molecules or two H2A molecules (Suto et al., 2000).

Studies in several organisms have contributed to our current understanding of H2A.Z function. In mammals, H2A.Z localizes with Hp1 α (heterochromatin protein 1) to pericentric heterochromatin during early development (Rangasamy et al., 2003). Furthermore, Hp1 α and H2A.Z cooperate to help form higher-order chromatin (Fan et al., 2004), suggesting roles for H2A.Z in hetero-chromatin compaction. Studies in flies present a complex picture; the fly ortholog, termed H2AvD, appears to be a hybrid of two mammalian H2A variants (Redon et al., 2002). On polytene chromosomes, H2AvD displays a widespread nonrandom distribution, though it is notably absent from loci that are the most highly transcribed (Leach et al., 2000). In addition, although H2AvD is present at modest levels at certain heatshock genes, heat-shock conditions reduced H2AvD occupancy (Leach et al., 2000). In *Tetrahymena*, H2A.Z is associated with active chromatin (Stargell et al., 1993), and extensive studies on its charged N-terminal tail show that charge neutralization via acetylation is critical for H2A.Z function (Ren and Gorovsky, 2001). Collectively, H2A.Z has complex roles in both transcriptional regulation and chromosome metabolism.

Studies in yeast support broad roles for Htz1 in transcriptional regulation and chromosome metabolism (Kamakaka and Biggins, 2005). Htz1 occupies the promoter regions of the *GAL1-10* and *PHO5* genes during repression; although an *htz1* Δ in isolation has no impact on their activation, combining *htz1* Δ with mutations in chromatin remodeling complexes confers a significant activation defect to these genes (Santisteban et al., 2000). Furthermore, loss of Htz1 leads to the silencing of genes near telomeres due to the propagation of SIR proteins into telomere-proximal regions (Meneghini et al., 2003; Zhang et al., 2004), suggesting that Htz1 provides an anti-silencing function. Htz1 function may extend beyond transcription to genomic stability and DNA repair, as *htz1* Δ mutants show chromosomal loss defects and sensitivity to various DNA-damaging agents (Kobor et al., 2004; Krogan et al., 2004; Mizuguchi et al., 2004). In summary, these studies suggest a positive role for Htz1 in gene activation and additional roles in other chromosomal processes.

A central question in the biology of histone variants is how and where variant nucleosomes are assembled. The identification of the SWR1 histone exchange complex represented a major advance; SWR1 removes H2A-H2B dimers and replaces them with Htz1-H2B dimers (Kobor et al., 2004; Krogan et al., 2003; Mizuguchi et al., 2004). Deposition of Htz1 in vivo requires the catalytic subunit of the complex, Swr1, at the limited loci examined (mainly telomeric). Deposition at telomeres also requires the SWR1 component Yaf9, a yeast ortholog of the human AF9 and ENL proteins involved in acute leukemias (Zhang et al., 2004). Currently, little is understood about how SWR1 is targeted to particular genes and whether chromatin features like acetylation assist in targeting. Here, Bdf1 may help link SWR1 to acetylated chromatin; Bdf1 bears two bromodomains (acetyl-lysine binding domains) and binds acetylated H3 and H4 in vitro (Ladurner et al., 2003; Matangkasombut and Buratowski, 2003). Bdf1 is a member of SWR1 complex (as well as TFIID; Kobor et al., 2004; Krogan et al., 2003; Matangkasombut et al., 2000) and therefore may target the SWR1 complex to acetylated regions. Yeast also

contain a paralog of Bdf1, termed Bdf2, which interacts with TFIID and also with histone H3 and H4 tails but in an acetylation-independent manner (Matangkasombut et al., 2000; Matangkasombut and Buratowski, 2003). Although Bdf1 and Bdf2 interact physically (Gavin et al., 2002), a clear link between Bdf2 and the SWR1 complex has not been established. Still, the presence of a double bromodomain protein in SWR1 raises the interesting question of whether histone acetylation assists in Htz1 deposition.

Here, we address the following questions regarding the genome-wide strategy for Htz1 utilization: (1) Where is Htz1 localized in the genome, and are SWR1 members responsible for all Htz1 deposition? (2) What are the features of occupied sites with respect to acetylation, activators, promoter features, and gene programs/classes? (3) Is the main function of Htz1 to form an antisilencing boundary at telomeres? (4) Does Htz1 redistribute when transcriptional programs are altered? (5) Do occupied genes rely on Htz1 for their full activation or repression? (6) Are nucleosomes bearing Htz1 more or less stable than those containing H2A, and does this contribute to gene regulation? As nucleosome deficiency and loss are a central feature of promoter regulation (Bernstein et al., 2004; Lee et al., 2004), this last question is of particular interest. Our work suggests that Htz1 is deposited at the promoters of many repressed/basal genes throughout the genome; Htz1 occupancy correlated with histone acetylation at particular residues, and occupancy is partially reliant on the Gcn5 histone acetyltransferase (HAT). Importantly, we show preferential loss of Htz1 (in comparison to H2A or H3) from chromatin *in vivo* in response to activation and *in vitro* under conditions of moderate ionic strength, suggesting that Htz1-bearing nucleosomes (possibly in combination with acetylation) are unstable and susceptible to loss. Taken together, these results reveal a strategy for the use of this histone variant—certain repressed promoters are marked with fragile chromatin that is susceptible to histone loss, thereby facilitating the binding of transcription factors.

Results

Genome-Wide Localization of Htz1 and the SWR1 Complex

Htz1 occupancy genome-wide was determined in a haploid *S. cerevisiae* strain during asynchronous growth in rich media containing glucose. To enable Htz1 isolation, a derivative encoding HA-tagged Htz1 (HA-Htz1) was integrated at the *HTZ1* genomic locus. To identify Htz1-occupied sites, we isolated genomic DNA fragments (average length of 350 bp) associated with Htz1 by chromatin immunoprecipitation (ChIP) using an α HA (12CA5) antibody. ChIP-enriched fragments and input control DNA were labeled with fluorescent dyes (Cy5 and Cy3, respectively) and used to probe a DNA array of the *S. cerevisiae* genome. Our array consists of the entire genome parsed into two types of segments, open reading frames (ORFs) and intergenic regions (IGRs). ORFs and IGRs were spotted on separate slides, requiring their separate analysis and presentation. For each segment, a normalized Cy5/Cy3 ratio was determined, which provided a measurement of Htz1 occupancy at each segment. We also applied percentile rank analysis (a common alternative method) to depict relative Htz1 occupancy. Here, Htz1 occupancy measurements (Cy5/Cy3 ratios) were ordered (from highest to lowest) and then sorted into 100 bins, with each bin containing 1% of the total number of segments. Segments of highest Htz1 enrichment were assigned to the one hundredth percentile rank bin and those of lowest enrichment to the first percentile rank bin. Next, the median percentile rank (MPR) of three independent replicate experiments was determined for each segment. Through this analysis, the median MPR (mMPR) can be determined for any set of genes or chromosomal elements and compared to any other set of genes/elements. The full Htz1 occupancy dataset is available in the Supplemental Data available with this article online.

Htz1 occupancy was highly reproducible and specific; three biological replicates yielded Pearson correlation coefficients (r) of ≥ 0.94 (Figure 1A), which depended on tagged Htz1 (Figure 1B). Enrichment of Htz1-occupied segments was also efficient; plots depicting the

distribution of ChIP enrichment ratios were broad, reflecting a consistent nonrandom localization pattern of Htz1 (Figures 1C and 1D). These three Htz1 ChIP replicates generated an average of 1743 segments (ORF, 764; IGR, 979) with at least a 2-fold enrichment (\log_2 value ≥ 1 ; Figures 1C and 1D), whereas only 124 segments (ORF, 33; IGR, 91) were generated from untagged replicates.

The catalytic component of the SWR1 complex, Swr1, was also localized during asynchronous growth in rich media. A tagging construct was integrated into the 3' end of the chromosomal *SWR1* gene to encode a myc-tagged Swr1 protein (Swr1-Myc). Swr1-Myc occupancy was reproducible ($r \geq 0.62$; data not shown) but of low efficiency; only 26 IGRs averaged at least a 2-fold enrichment (\log_2 value ≥ 1), though ~ 200 IGRs were reproducibly enriched over 1.5-fold. The full Swr1 occupancy dataset is available in the Supplemental Data. Htz1 and Swr1 coincidence was clear and significant, as revealed in MPR comparisons (Figure 1E) and Venn diagram analyses ($p = 5 \times 10^{-26}$; Figure 1F). Notably, the promoter with the highest Swr1-Myc occupancy is the *SWR1* promoter, raising the possibility for a regulatory loop involving Htz1 deposition.

Specific Htz1 Deposition Requires Swr1 and Is Strongly Promoted by Yaf9 Genome-Wide

The pattern of Htz1 deposition at specific loci genome-wide requires Swr1, as HA-Htz1 occupancy in *swr1* Δ mutants was indistinguishable from untagged replicates (Figure 1G). Furthermore, strains lacking the Yaf9 component of SWR1 complex display dramatic reductions in specific Htz1 occupancy genome-wide (Figure S1). However, percentile rank analysis showed that the same loci occupied in the wt strain are occupied in the *yaf9* Δ strain but at a reduced level. Thus, Yaf9 is likely more important for the mechanism of Htz1 deposition than the targeting of SWR1.

Htz1 Occupancy at Particular Chromosome Elements

In higher eukaryotes, H2A variants such as H2A-Bdb and Macro-H2A cluster to particular chromosomal regions (Chadwick and Willard, 2001; Costanzi et al., 2000). However, we observe no significant clustering of Htz1 (data not shown). Htz1 displays average occupancy at the available class of centromere and centromere-adjacent segments (mMPR 51%) and also at the predicted set of autonomously replicating sequences (mMPR 53%) (Wyrick et al., 2001). Furthermore, we find that telomere-proximal IGRs (within 20 kb of the telomere) show average occupancy (mMPR 50%), an unexpected result considering the strong downregulation of genes near telomeres in *htz1* Δ cells (Meneghini et al., 2003; see Discussion). Notably, Htz1 is deficient at certain loci; Pol I genes show an mMPR of 38%, segments flanking Pol III genes an mMPR of 39%, and tRNAs themselves an mMPR of 21%.

Htz1 Occupies Promoters Genome-Wide

To examine whether Htz1 generally occupies promoters, we separated IGRs into three classes: (1) nonpromoters, which are flanked by the 3' end of two ORFs, (2) single promoters, which are flanked by one ORF 5' end and one ORF 3' end, and (3) double promoters, which are flanked by two ORF 5' ends. Htz1 has a striking preference for promoters (Figures 2A and 2B), whereas TAP-tagged H2A displayed a weak preference for the alternative class, nonpromoters (Figures 2C and 2D). Highly occupied promoters likely bear (on average) only one Htz1-containing nucleosome, as these promoters are not detectably H2A deficient (data not shown).

To determine quantitatively whether Htz1 preferentially occupies the promoter or the ORF, we compared Htz1 occupancy at ten genes by quantitative PCR (qPCR). At all ten genes, higher occupancy was observed over the promoter region (Figure 2E). Tiling analysis of six promoters revealed that the resolution of our Htz1 occupancy measurements was ~ 300 bp and that the peaks of Htz1 occupancy ranged from ~ 100 to ~ 400 bp upstream of the ATG start codon,

which would correspond to the nucleosome at the -1, -2, or -3 position of the promoter (Figure S2). Yeast promoters have been classified as either TATA-containing or TATA-less (Basehoar et al., 2004), and for the two TATA-containing promoters tested (*YOR285W* and *YDL218W*), the peak of Htz1 occupancy was either at or adjacent to the TATA box (Figure S2).

The promoter specificity observed in our qPCR analyses raised the possibility that the detection of Htz1 at ORFs might simply reflect proximity to a highly enriched promoter. Consistent with this notion, for highly enriched ORFs the mMPR of their flanking promoters was 80% whereas the mMPR of their flanking nonpromoters was 31%. This bias strongly suggests that ORFs appear occupied in the genome-wide ChIP method due to their proximity to highly occupied promoters. Thus, all subsequent analyses will focus on IGRs.

Htz1 Occupancy at Gene Classes

We observe Htz1 at hundreds of promoters with broad roles in cell regulation. However, significant enrichment was observed at the following particular gene classes: mitochondrial ribosomal protein genes (mRPGs, mMPR 84%), genes for ribosome biogenesis (mMPR 88%), genes encoding members of RNA polymerase III (mMPR 88%), and mitochondrial tRNA synthetases (mMPR 81%). Two classes of genes are notably deficient in Htz1: cytoplasmic ribosomal protein genes (cRPGs, mMPR 16%) and translation elongation factors (mMPR 24%), two gene classes with exceptionally high transcription rates. Thus, mRPGs and cRPGs are the most and least occupied gene classes, respectively. However, whereas mRPGs show typical levels of H2A (mMPR 50%), H2A is virtually absent at cRPG promoters (mMPR 10%; Figure S3), in keeping with the observations of others that cRPG promoters are deficient in histone H3 (Bernstein et al., 2004; Lee et al., 2004). Notably, mRPGs are more highly transcribed in the presence of a nonfermentable carbon source, whereas cRPGs are more highly transcribed in the presence of a fermentable carbon source (Shamji et al., 2000), raising the possibility that Htz1 may be utilized selectively for the mRPG program.

Htz1 Occupancy Correlates with Particular Transcription Factors

The targeting of Htz1 deposition involves SWR1 recruitment, which may be guided by transcriptional regulators or chromatin structural elements/modifications. To identify transcription factor candidates, we examined correlations between Htz1 occupancy and transcription factor occupancy of promoters (Harbison et al., 2004). We find a statistically significant overlap with at least four transcription factors: Abf1 ($p = 6.63 \times 10^{-15}$), Fkh1 ($p = 1.27 \times 10^{-4}$), Reb1 ($p = 6.77 \times 10^{-6}$), and Pho4 ($p = 1 \times 10^{-3}$). For example, Htz1 occupancy is high at 80 out of a total of 157 Abf1 targets, including genes encoding mRPGs, members of RNA Pol III, and nuclear pore components. A list of genes occupied by these transcription factors and Htz1 is provided in Table S3.

Htz1 and Bdf1 Preferentially Occupy TATA-less Promoters

Gene promoters have been classified as either TATA-containing or TATA-less. Interestingly, transcription of TATA-containing genes is predominantly affected by mutations in SAGA components, whereas TATA-less gene transcription is predominantly affected by mutations in TFIID components (Basehoar et al., 2004; Huisinga and Pugh, 2004). However, both complexes utilize TBP (the TATA binding protein) for transcriptional initiation. Each complex also contains unique members (i.e., Spt3 for SAGA, Bdf1 for TFIID) which have been localized by genome-wide ChIP (Kurdistani et al., 2004; Zanton and Pugh, 2004). Our analyses of these datasets reveal a clear negative correlation between Bdf1 occupancy and the presence of a consensus TATA-box in the promoter, whereas Spt3 occupancy is weakly positively correlated (Figures 3A and 3B; only 19% of yeast promoters are TATA containing (Basehoar et al., 2004). Bdf1 is a substoichiometric (or loosely associated) member of the SWR1 complex (Kobor et al., 2004; Krogan et al., 2003), raising the possibility that Bdf1 may help recruit

SWR1/Htz1 to TATA-less promoters. Consistent with this notion, we observe a strong positive correlation between Bdf1 occupancy and Htz1 occupancy (Figure 3C), whereas a weak negative correlation is observed with Spt3 occupancy (Figure 3D). Furthermore, we observe a clear negative correlation between Htz1 occupancy and the presence of a TATA box, similar to our observations with Bdf1 (Figure 3E). Taken together, Bdf1 and Htz1 occupy a largely overlapping set of promoters, with a clear bias toward TATA-less promoters.

Htz1 Occupancy Correlates with Particular Histone Acetylation Patterns

Htz1 occupancy correlates with relative acetylation levels at particular histone residues at IGRs (Kurdistani et al., 2004), displaying a strong positive correlation with acetylation of the H3 tail at lysine 14 (H3K14ac) and a strong negative correlation with H3K27ac (Table 1). Also apparent was positive correlation with H2AK7ac and H4K8ac and negative correlation with H3K9ac levels. Whereas the absolute levels of promoter H3K14ac are not well correlated with transcriptional frequency, H3K27ac levels are well correlated with transcription (Kurdistani et al., 2004), suggesting that Htz1 occupies genes in their repressed/basal states, which we investigate further below.

Although Htz1 occupancy correlates with particular acetylation patterns, no single modification appears solely responsible for directing deposition, as specific Htz1 deposition patterns are not dramatically altered in strains bearing amino acid replacement(s) at key sites of modification in histones H3 or H4: H3K14G, H3K14Q, H3K14R, H4K16R, H4K16Q, H4K8+16R, H4K5+12R, H3K4A, H3K4R, or in a *set1* Δ strain (data not shown). However, in each mutant strain, particular genes can be identified with dramatic reductions in Htz1 occupancy (data not shown). This raises the possibility that different promoter contexts might impose reliance on a specific modification for deposition.

Strains Lacking Gcn5 or Bdf1 Show Significant Reductions in Htz1 Occupancy

Htz1 occupancy correlated with H3K14ac but did not require this modification. Therefore, we reasoned that Htz1 occupancy might involve acetylation by HAT enzymes that have H3K14 among their preferred substrates and tested Gcn5 and Sas3 (members of the SAGA/SLIK/ADA and NuA3 HAT complexes, respectively). We observed clear alterations in Htz1 occupancy genome-wide in strains lacking Gcn5; IGRs that are highly occupied by Htz1 in the wt strain fall an average of 10-15 percentile ranks in a *gcn5* Δ strain (Figure 4A). The loss of Sas3 also reduces Htz1 occupancy, though to a much lesser extent (Figure 4B). Thus, Htz1 occupancy shows a significant reliance on Gcn5 at many loci.

SWR1 complex contains Bdf1, a protein that binds to acetylated histone tails and is well correlated with Htz1 occupancy (Figure 3C). Therefore, we tested the extent to which Htz1 occupancy relies on Bdf1 (or its paralog Bdf2) by examining Htz1 occupancy in *bdf1* Δ and *bdf2* Δ strains. Here, we utilized a polyclonal antibody to Htz1 for ChIP analysis; ChIP efficiencies and Htz1 locations determined with this antibody (in wt cells) were highly reproducible ($r = 0.89$) and very similar to those determined in HA-Htz1-tagged strains ($r = 0.88$). Interestingly, loss of Bdf1 conferred a reduction of Htz1 occupancy averaging 10-15 percentile ranks at genes bearing high levels of Htz1 in wt cells (Figure 4C). In counter distinction, the loss of Bdf2 altered Htz1 occupancy only slightly (Figure 4D). Thus, Htz1 occupancy relies on Bdf1 function at many loci.

To quantify these effects, we performed qPCR at the ten promoters we examined previously for promoter specificity. Consistent with the genome-wide trends, significant reductions were observed at most of these loci in strains lacking either Gcn5 or Bdf1, whereas reductions were observed at fewer loci (and were generally of lesser magnitude) in strains lacking Sas3 or Bdf2 (Figure 4E). However, although Htz1 occupancy is reduced at many promoters in cells lacking

Bdf1 or Gcn5, we did not observe a bias with respect to the presence or absence of a TATA box (data not shown). Taken together, Htz1 occupancy shows a significant reliance on Gcn5 and on Bdf1, suggesting that these factors participate in the acetylation and acetyl-recognition of promoter targets for Htz1 replacement, but these factors alone do not confer the bias toward TATA-less promoters.

Htz1 Occupancy Is Negatively Correlated with Transcription Rate

To understand how Htz1 influences transcription, we examined whether Htz1 localizes to active or repressed gene promoters. Here, we compared Htz1 occupancy (or H2A occupancy) at promoters to the transcription rate of their respective ORFs (Holstege et al., 1998). We restricted our analysis to single promoters, which allowed the unambiguous assignment of a promoter IGR to its linked ORF. Interestingly, Htz1 occupancy was clearly negatively correlated with transcription rate (Figure 5A). In counter distinction, H2A was only weakly negatively correlated (Figure 5B). This raised the possibility that Htz1 might be lost/ejected from promoters during activation, to a greater extent than H2A.

Activation Promotes Htz1 Loss, Whereas Repression Promotes Htz1 Acquisition

The experiments above prompted us to test whether Htz1 exhibits dynamic redistribution in response to transcriptional changes. Here, we examined the changes in Htz1 occupancy resulting from heat shock (HS) or diauxic shift, which each alter the transcription of hundreds of genes. For simplicity, we will refer to “activated” and “repressed” promoters in relation to the transcriptional response of their linked ORF. Cultures were shifted from 25°C to 37°C for 30 min (HS) and then returned to 25°C for 30 min (recovery). For each condition, we compared changes in gene expression to changes in Htz1 occupancy genome-wide. Remarkably, activated single promoters lost Htz1, whereas repressed single promoters acquired Htz1, with occupancy changes inversely proportional to transcriptional changes (Figure 5C). For example, genes that are activated 8-fold ($\log_2 = 3$ on the x axis, Figure 5C) display greater than a 2-fold average decrease in their mMPR measurement of Htz1 occupancy ($\log_2 -1.1 = -2.2$ -fold). Furthermore, recovery from HS largely restored Htz1 occupancy to initial values, showing that these changes are both dynamic and reversible. With H2A, the trend was similar, but the magnitude was greatly reduced (Figure 5D). This behavior may be general, as the diauxic shift provided a similar response; Htz1 was lost at activated genes and gained at repressed genes (Figure 5E). We then tested the relationship between Htz1 occupancy and TBP occupancy. Interestingly, we found that TBP occupancy at IGRs (omitting Pol III genes; Roberts et al., 2003) and Htz1 occupancy are inversely correlated (Figure 5F).

We next examined a particular gene promoter activated by HS that initially bore high levels of Htz1. We chose the promoter for *YDC1* (*pYDC1*) which encodes a ceramidase required for HS response (see Figure S2 for diagram). To examine the kinetics of Htz1 loss, we performed a HS time course. Remarkably, at *pYDC1* Htz1 is lost rapidly and to a much greater extent than either H2A or H3 (Figure 6A). Moreover, the kinetics suggested that Htz1 loss was not replication dependent. Taken together, promoters bearing high levels of Htz1 that are activated by HS rapidly lose Htz1 during activation.

Htz1 Promotes Activation, Not Repression, of Occupied Promoters

Next, we examined the extent to which genes bearing Htz1 at their promoter rely on Htz1 for regulation. Here, we subjected wt and *htz1Δ* cells to HS and performed transcription profiling. Importantly, we observed an attenuation of activation of a particular class of genes; those genes that in wt cells lose the highest proportion of Htz1 (Figure 6B). For example, genes normally activated about 4-fold in wt ($\log_2 = 2$, on the y axis) are attenuated to 2.8-fold activation ($\log_2 = 1.5$, on the y axis) in *htz1Δ* cells (Figure 6B, region 1). In keeping with this overall trend, *YDC1* activation is attenuated almost 2-fold in *htz1Δ* cells during the early response to

HS, consistent with the kinetics of Htz1 loss (Figure 6C). In contrast, genes repressed following HS show no reliance on Htz1 for their repression (Figure 6B, region 2). Taken together, these results suggest that Htz1 is deposited at promoters during repression but is not required to establish the repressed/basal state (at least for the HS response). Instead, it appears to poise the promoter to facilitate activation through ejection/loss during a later activation program.

Htz1 Is More Susceptible to Release from Purified Yeast Chromatin Than H2A or H3

Next, we sought a biochemical basis for our observation that Htz1 is lost/ejected from promoters to a greater extent than is H2A during activation. One clear possibility is that nucleosomes bearing Htz1 are less stable than their H2A-containing counterparts in yeast chromatin, rendering them more susceptible to ejection during activation. To examine this, we performed a standard yeast chromatin preparation and subjected the chromatin pellet to salt washes of increasing ionic strength. Remarkably, HA-Htz1 is largely removed under conditions of moderate ionic strength and almost fully removed under conditions of high ionic strength. In contrast, little or no H2A-TAP or H3 is removed under either condition (Figure 6D). This behavior is not conferred by the epitope tags on Htz1 or H2A, as identical results were obtained with chromatin purified from an untagged wt strain examined with polyclonal Htz1 or H2A antibodies (data not shown). Taken together, nucleosomes bearing Htz1 present in yeast chromatin are less stable than their canonical counterparts; this property may serve to mark repressed/basal promoters with a nucleosome susceptible to histone loss during activation.

Discussion

Cells utilize histone variants to construct specialized chromatin structures that assist in transcriptional regulation, DNA repair, and chromosome segregation (Kamakaka and Biggins, 2005). Although mammals have many histone variants, only two are shared among all eukaryotes: a histone H3 variant (specialized for centromere function) and an H2A variant, termed H2A.Z in mammals and Htz1 in *Saccharomyces cerevisiae*. Numerous studies have established roles for H2A.Z/Htz1 in transcriptional regulation, chromosome structure, and DNA repair (see Introduction). However, the studies involving transcriptional regulation have been limited to an examination of Htz1 function at relatively few genes and have not provided a clear mechanism for the use of Htz1 in gene regulation. Our studies examined Htz1 occupancy and dynamics genome-wide in response to environmental changes and also in strains lacking candidate regulators of Htz1 function. The results motivated a biochemical analysis of Htz1 in purified chromatin which, together with previous studies, suggest a strategy and mechanism for Htz1 in gene regulation (Figure 7).

Htz1 Occupancy at Chromosomal Elements

Htz1 is not highly enriched at centromeres and predicted origins of replication. However, as we utilized asynchronous cultures, cell cycle-dependent association of Htz1 remains to be examined. Furthermore, loci bearing the “average” level of Htz1 may still utilize Htz1 for their regulation. Strains lacking Htz1 show the physical spreading of silencing factors (SIR proteins) from certain telomeres into telomere-proximal genes (Zhang et al., 2004), imposing transcriptional silencing (Meneghini et al., 2003). This raised the possibility that Htz1 levels at telomeres might be exceptionally high in order to build an antisilencing “boundary.” However, we did not observe enrichment of Htz1 in telomere-proximal regions (mMPR of 50%, within 20 kb). Interestingly, cells bearing H4K16 substitutions display SIR-dependent silencing of telomere-proximal genes (Kimura et al., 2002; Suka et al., 2002) but retain Htz1 occupancy at those loci (data not shown), suggesting that SIR proteins can spread through Htz1-occupied genes deficient in H4 acetylation. Thus, Htz1 is likely one of many factors that contribute to antisilencing, with acetylation of prime importance.

Htz1 Generally Occupies Pol II Promoters and Requires Swr1 for Promoter Deposition

Our studies revealed Htz1 at the promoters of hundreds of Pol II genes. Some promoter occupancy was expected based on previous studies (Larochelle and Gaudreau, 2003; Santisteban et al., 2000), but the wide scope and Pol II specificity revealed in our analysis firmly establishes Pol II promoter occupancy as a general property of Htz1. Notably, we observe significantly higher levels of Htz1 at TATA-less promoters, which preferentially utilize TFIID for initiation. At present, the factors or chromatin patterns directing this bias have not been identified, but the observation remains compelling. As Htz1 deposition at promoters genome-wide requires Swr1, and as Swr1 largely colocalizes with Htz1 on chromatin, SWR1 complex is established as the primary (if not the sole) factor directing specific localized Htz1 deposition (Figure 7). Thus, the central questions regarding Htz1 deposition now focus on understanding how SWR1 is recruited to Pol II promoters and the nature of the bias for TATA-less promoters.

Roles for Bdf1, Gcn5, and Histone Acetylation in Promoting Htz1 Occupancy

SWR1 recruitment could involve: (1) physical interactions between SWR1 and DNA sequence-specific transcriptional regulators, (2) physical interactions between SWR1 and promoter binding initiation factors (such as TFIID or SAGA components), or (3) recognition of modified histones by Bdf1 or other SWR1 components. Our work addresses aspects of all three processes. First, our occupancy correlations revealed four transcription factors as candidate recruiters of SWR1 (Table S3), which require testing. Second, we show that Bdf1 (which bears two bromodomains with a relatively broad range of acetylation recognition) is required for full Htz1 deposition at many loci. Third, we provide three links among Bdf1, histone acetylation, and Htz1 deposition: the aforementioned involvement of Bdf1, the reliance on Gcn5 for full Htz1 occupancy at many loci, and the correlation between Htz1 occupancy and acetylation at particular histone residues (Figure 7). Here, we emphasize that our correlations with acetylation do not define a single chromatin state that “codes” for Htz1 deposition; not all highly occupied IGRs bear all correlated marks. Furthermore, as significant Htz1 deposition occurs in cells lacking Bdf1 or Gcn5, other HATs and other factors that recognize modified histone tails must contribute to acetylation patterns and their recognition. Therefore, our data is consistent with Gcn5 contributing (along with other HATs) to a promoter acetylation pattern recognized by Bdf1 and other factors that promote Htz1 deposition. In addition, transcription factors may work together with HATs and Bdf1 to recruit SWR1 to particular promoters.

Htz1 Dynamics

A central issue in chromatin biology is how histone/nucleosome occupancy affects transcription. As nucleosomes can block the binding of transcriptional regulators and machinery, factors that mediate histone loss could serve general roles in the exposure of promoter sequences. Remarkably, nucleosome deficiency is a general property of yeast promoters (Bernstein et al., 2004; Lee et al., 2004), and the activation process promotes histone loss (Boeger et al., 2003; Deckert and Struhl, 2001; Reinke and Horz, 2003). Consistent with these trends, activation promotes Htz1 loss and repression its deposition, an observation consistent with previous studies of Htz1 at *PHO5* and *GALI-10* (Larochelle and Gaudreau, 2003; Santisteban et al., 2000). Our studies establish this as a general property of Htz1. Importantly, we show that Htz1 loss or acquisition is of greater magnitude than H2A, suggesting Htz1 as a dynamic variant. This dynamic nature likely contributes to the full and rapid activation of occupied genes, as attenuated activation (but not repression) in *htz1*Δ strains is observed primarily at genes highly occupied in wt cells (Figure 6B). Taken together, our data suggest Htz1 as a general activator that is deposited during repression, whose loss promotes activation.

Htz1 Susceptibility to Loss as a Mechanism to Expose Promoter DNA

We observe nearly quantitative loss of Htz1 from purified yeast chromatin in ionic conditions that cause little or no release of histone H2A or H3, providing biochemical evidence that Htz1 nucleosomes are less stable than H2A nucleosomes in purified yeast chromatin. Structural studies suggest subtle differences at the dimer-tetramer interface that could confer relative instability (Suto et al., 2000). However, two careful biophysical studies of recombinant H2A.Z nucleosomes came to opposite conclusions, with one study showing increased stability (Park et al., 2004) while another showed decreased stability (Abbott et al., 2001) relative to H2A nucleosomes. However, our studies involved an analysis of Htz1 in chromatin purified from yeast cells. The instability we observe in chromatin might be an intrinsic property of nucleosomes bearing Htz1, a property of the modifications present on these nucleosomes (or in the region, Table 1), or a combination of both. We note that as Htz1 is present at only ~5% of the levels of H2A, our data does not definitively determine whether the entire Htz1 nucleosome is ejected or whether only the Htz1-H2B dimers are removed, leaving a resident H3-H4 tetramer. This is also true for our in vivo assessments of Htz1 loss; as the DNA fragments isolated in our ChIP experiments range from 150-600 bp, the specific loss of one Htz1 nucleosome in an array with other H2A nucleosomes would result in only modest reductions in H3 levels. Thus, only relative loss can be assessed.

One unresolved question is how Htz1 loss is coupled to activation. One possibility is that a chromatin remodeler could actively eject Htz1 nucleosomes, with particular tail modification patterns helping to guide the ejection process. Thus, a speculative model consistent with our data is that Htz1 nucleosomes in yeast chromatin are more susceptible to ejection than their canonical counterparts when acted upon by remodeling complexes, due to a combination of intrinsic properties and modifications (Figure 7). Ejection could facilitate the binding of TBP or the binding of transcriptional activator proteins, either of which would promote the activation process. Our demonstration of Htz1 dynamics and instability provides a mechanistic basis for the loss of an Htz1 nucleosome and the exposure of promoter DNA during activation.

Experimental Procedures

Yeast Strains, Media, and Genetic Methods

Full genotypes for strains are provided in Table S1. Isolation of strains, genetic methods, and preparation of media followed standard procedures.

Heat Shock and Diauxic Shift

For HS, cells were grown in YPD at 25°C to an OD₆₀₀ of ~0.8, and a fraction of the culture was taken as a control sample (T = 0, no HS). The remainder were collected and resuspended in YPD prewarmed at 37°C. Growth was continued at 37°C for 30 min and samples were collected (HS). Then the culture was shifted back to 25°C for 30 min and samples were collected (recovery). For the HS time course, cultures at the indicated time points were split for expression profiling and ChIP analysis (by qPCR). For diauxic shift experiments, cells were grown in YPD at 30°C to an OD₆₀₀ of ~0.3 (T = 0), and samples were collected every 2 hr for 24 hr.

RNA Preparation, ChIP, qPCR, and Microarray Analysis

Procedures were performed as described in Roberts et al. (2003), with details provided in the Supplemental Experimental Procedures. Primer sets for qPCR analysis are provided in Table S2.

Chromatin Preparation

A detailed description of the chromatin preparation is provided in the Supplemental Experimental Procedures. In brief, cells were collected during log phase growth and spheroplasted using glucosylase. Nuclei were separated on a sucrose cushion; membranes were extracted by detergent. The chromatin pellet was then isolated via centrifugation and subjected to salt extraction using buffers of increasing stringency. Samples were analyzed by SDS-PAGE, Coomassie blue staining, and Western analysis.

Supplementary Material

Refer to Web version on PubMed Central for supplementary material.

Acknowledgments

This work was supported by the Howard Hughes Medical Institute (support of B.R.C. and all reagents), the Huntsman Cancer Institute (for Microarray Resources), the National Institutes of Health (GM60415 [to B.R.C.] for support of H.Z. and D.N.R., and CA24014, for support of core facilities). We thank E. O'Shea, J.S. Weissman, M. Smith, and S. Dent for strains and plasmids. We also thank J. Lieb, S. Mango, M. Gordon, J. Wittmeyer, and D. Richardson for helpful comments and B. Dalley and Q. Yang for ChIP sample processing.

References

- Abbott DW, Ivanova VS, Wang X, Bonner WM, Ausio J. Characterization of the stability and folding of H2A.Z chromatin particles: implications for transcriptional activation. *J. Biol. Chem* 2001;276:41945–41949. [PubMed: 11551971]
- Adam M, Robert F, Laroche M, Gaudreau L. H2A.Z is required for global chromatin integrity and for recruitment of RNA polymerase II under specific conditions. *Mol. Cell. Biol* 2001;21:6270–6279. [PubMed: 11509669]
- Ahmad K, Henikoff S. Histone H3 variants specify modes of chromatin assembly. *Proc. Natl. Acad. Sci. USA* 2002;99(Suppl 4):16477–16484. [PubMed: 12177448]
- Basehoar AD, Zanton SJ, Pugh BF. Identification and distinct regulation of yeast TATA box-containing genes. *Cell* 2004;116:699–709. [PubMed: 15006352]
- Bernstein BE, Liu CL, Humphrey EL, Perlstein EO, Schreiber SL. Global nucleosome occupancy in yeast. *Genome Biol* 2004;5:R62. [PubMed: 15345046]
- Boeger H, Griesenbeck J, Strattan JS, Kornberg RD. Nucleosomes unfold completely at a transcriptionally active promoter. *Mol. Cell* 2003;11:1587–1598. [PubMed: 12820971]
- Chadwick BP, Willard HF. A novel chromatin protein, distantly related to histone H2A, is largely excluded from the inactive X chromosome. *J. Cell Biol* 2001;152:375–384. [PubMed: 11266453]
- Costanzi C, Stein P, Worrall DM, Schultz RM, Pehrson JR. Histone macroH2A1 is concentrated in the inactive X chromosome of female preimplantation mouse embryos. *Development* 2000;127:2283–2289. [PubMed: 10804171]
- Deckert J, Struhl K. Histone acetylation at promoters is differentially affected by specific activators and repressors. *Mol. Cell. Biol* 2001;21:2726–2735. [PubMed: 11283252]
- Fan JY, Rangasamy D, Luger K, Tremethick DJ. H2A.Z alters the nucleosome surface to promote HP1 α -mediated chromatin fiber folding. *Mol. Cell* 2004;16:655–661. [PubMed: 15546624]
- Gavin AC, Bosche M, Krause R, Grandi P, Marzioch M, Bauer A, Schultz J, Rick JM, Michon AM, Cruciat CM, et al. Functional organization of the yeast proteome by systematic analysis of protein complexes. *Nature* 2002;415:141–147. [PubMed: 11805826]
- Harbison CT, Gordon DB, Lee TI, Rinaldi NJ, Macisaac KD, Danford TW, Hannett NM, Tagne JB, Reynolds DB, Yoo J, et al. Transcriptional regulatory code of a eukaryotic genome. *Nature* 2004;431:99–104. [PubMed: 15343339]
- Henikoff S, Ahmad K, Platero JS, van Steensel B. Heterochromatic deposition of centromeric histone H3-like proteins. *Proc. Natl. Acad. Sci. USA* 2000;97:716–721. [PubMed: 10639145]

- Henikoff S, Furuyama T, Ahmad K. Histone variants, nucleosome assembly and epigenetic inheritance. *Trends Genet* 2004;20:320–326. [PubMed: 15219397]
- Holstege FC, Jennings EG, Wyrick JJ, Lee TI, Hengartner CJ, Green MR, Golub TR, Lander ES, Young RA. Dissecting the regulatory circuitry of a eukaryotic genome. *Cell* 1998;95:717–728. [PubMed: 9845373]
- Huisinga KL, Pugh BF. A genome-wide housekeeping role for TFIID and a highly regulated stress-related role for SAGA in *Saccharomyces cerevisiae*. *Mol. Cell* 2004;13:573–585. [PubMed: 14992726]
- Jackson JD, Falciano VT, Gorovsky MA. A likely histone H2A.F/Z variant in *Saccharomyces cerevisiae*. *Trends Biochem. Sci* 1996;21:466–467. [PubMed: 9009827]
- Jenuwein T, Allis CD. Translating the histone code. *Science* 2001;293:1074–1080. [PubMed: 11498575]
- Kamakaka RT, Biggins S. Histone variants: deviants? *Genes Dev* 2005;19:295–310. [PubMed: 15687254]
- Kimura A, Umehara T, Horikoshi M. Chromosomal gradient of histone acetylation established by Sas2p and Sir2p functions as a shield against gene silencing. *Nat. Genet* 2002;32:370–377. [PubMed: 12410229]
- Kobor MS, Venkatasubrahmanyam S, Meneghini MD, Gin JW, Jennings JL, Link AJ, Madhani HD, Rine J. A protein complex containing the conserved Swi2/Snf2-related ATPase Swr1p deposits histone variant H2A.Z into euchromatin. *PLoS Biol* 2004;2:e131. [PubMed: 15045029]10.1371/journal.pbio.0020131
- Krogan NJ, Keogh MC, Datta N, Sawa C, Ryan OW, Ding H, Haw RA, Pootoolal J, Tong A, Canadien V, et al. A Snf2 family ATPase complex required for recruitment of the histone H2A variant Htz1. *Mol. Cell* 2003;12:1565–1576. [PubMed: 14690608]
- Krogan NJ, Baetz K, Keogh MC, Datta N, Sawa C, Kwok TC, Thompson NJ, Davey MG, Pootoolal J, Hughes TR, et al. Regulation of chromosome stability by the histone H2A variant Htz1, the Swr1 chromatin remodeling complex, and the histone acetyltransferase NuA4. *Proc. Natl. Acad. Sci. USA* 2004;101:13513–13518. [PubMed: 15353583]
- Kurdistani SK, Tavazoie S, Grunstein M. Mapping global histone acetylation patterns to gene expression. *Cell* 2004;117:721–733. [PubMed: 15186774]
- Ladurner AG, Inouye C, Jain R, Tjian R. Bromodomains mediate an acetyl-histone encoded antisilencing function at heterochromatin boundaries. *Mol. Cell* 2003;11:365–376. [PubMed: 12620225]
- Larochelle M, Gaudreau L. H2A.Z has a function reminiscent of an activator required for preferential binding to intergenic DNA. *EMBO J* 2003;22:4512–4522. [PubMed: 12941702]
- Leach TJ, Mazzeo M, Chotkowski HL, Madigan JP, Wotring MG, Glaser RL. Histone H2A.Z is widely but nonrandomly distributed in chromosomes of *Drosophila melanogaster*. *J. Biol. Chem* 2000;275:23267–23272. [PubMed: 10801889]
- Lee CK, Shibata Y, Rao B, Strahl BD, Lieb JD. Evidence for nucleosome depletion at active regulatory regions genome-wide. *Nat. Genet* 2004;36:900–905. [PubMed: 15247917]
- Matangkasombut O, Buratowski S. Different sensitivities of bromodomain factors 1 and 2 to histone H4 acetylation. *Mol. Cell* 2003;11:353–363. [PubMed: 12620224]
- Matangkasombut O, Buratowski RM, Swilling NW, Buratowski S. Bromodomain factor 1 corresponds to a missing piece of yeast TFIID. *Genes Dev* 2000;14:951–962. [PubMed: 10783167]
- Meneghini MD, Wu M, Madhani HD. Conserved histone variant H2A.Z protects euchromatin from the ectopic spread of silent heterochromatin. *Cell* 2003;112:725–736. [PubMed: 12628191]
- Mizuguchi G, Shen X, Landry J, Wu WH, Sen S, Wu C. ATP-driven exchange of histone H2AZ variant catalyzed by SWR1 chromatin remodeling complex. *Science* 2004;303:343–348. [PubMed: 14645854]
- Owen-Hughes T. Colworth memorial lecture. Pathways for remodelling chromatin. *Biochem. Soc. Trans* 2003;31:893–905. [PubMed: 14505445]
- Park YJ, Dyer PN, Tremethick DJ, Luger K. A new fluorescence resonance energy transfer approach demonstrates that the histone variant H2AZ stabilizes the histone octamer within the nucleosome. *J. Biol. Chem* 2004;279:24274–24282. [PubMed: 15020582]
- Rangasamy D, Berven L, Ridgway P, Tremethick DJ. Pericentric heterochromatin becomes enriched with H2A.Z during early mammalian development. *EMBO J* 2003;22:1599–1607. [PubMed: 12660166]

- Redon C, Pilch D, Rogakou E, Sedelnikova O, Newrock K, Bonner W. Histone H2A variants H2AX and H2AZ. *Curr. Opin. Genet. Dev* 2002;12:162–169. [PubMed: 11893489]
- Reinke H, Horz W. Histones are first hyperacetylated and then lose contact with the activated PHO5 promoter. *Mol. Cell* 2003;11:1599–1607. [PubMed: 12820972]
- Ren Q, Gorovsky MA. Histone H2A.Z acetylation modulates an essential charge patch. *Mol. Cell* 2001;7:1329–1335. [PubMed: 11430834]
- Roberts DN, Stewart AJ, Huff JT, Cairns BR. The RNA polymerase III transcriptome revealed by genome-wide localization and activity-occupancy relationships. *Proc. Natl. Acad. Sci. USA* 2003;100:14695–14700. [PubMed: 14634212]
- Santisteban MS, Kalashnikova T, Smith MM. Histone H2A.Z regulates transcription and is partially redundant with nucleosome remodeling complexes. *Cell* 2000;103:411–422. [PubMed: 11081628]
- Shamji AF, Kuruvilla FG, Schreiber SL. Partitioning the transcriptional program induced by rapamycin among the effectors of the Tor proteins. *Curr. Biol* 2000;10:1574–1581. [PubMed: 11137008]
- Smith MM. Centromeres and variant histones: what, where, when and why? *Curr. Opin. Cell Biol* 2002;14:279–285. [PubMed: 12067649]
- Stargell LA, Bowen J, Dadd CA, Dedon PC, Davis M, Cook RG, Allis CD, Gorovsky MA. Temporal and spatial association of histone H2A variant hv1 with transcriptionally competent chromatin during nuclear development in *Tetrahymena thermophila*. *Genes Dev* 1993;7:2641–2651. [PubMed: 8276246]
- Suka N, Luo K, Grunstein M. Sir2p and Sas2p opposingly regulate acetylation of yeast histone H4 lysine16 and spreading of heterochromatin. *Nat. Genet* 2002;32:378–383. [PubMed: 12379856]
- Suto RK, Clarkson MJ, Tremethick DJ, Luger K. Crystal structure of a nucleosome core particle containing the variant histone H2A.Z. *Nat. Struct. Biol* 2000;7:1121–1124. [PubMed: 11101893]
- Wyrick JJ, Aparicio JG, Chen T, Barnett JD, Jennings EG, Young RA, Bell SP, Aparicio OM. Genome-wide distribution of ORC and MCM proteins in *S. cerevisiae*: high-resolution mapping of replication origins. *Science* 2001;294:2357–2360. [PubMed: 11743203]
- Zanton SJ, Pugh BF. Changes in genomewide occupancy of core transcriptional regulators during heat stress. *Proc. Natl. Acad. Sci. USA* 2004;101:16843–16848. [PubMed: 15548603]
- Zhang H, Richardson DO, Roberts DN, Utley R, Erdjument-Bromage H, Tempst P, Cote J, Cairns BR. The Yaf9 component of the SWR1 and NuA4 complexes is required for proper gene expression, histone H4 acetylation, and Htz1 replacement near telomeres. *Mol. Cell. Biol* 2004;24:9424–9436. [PubMed: 15485911]

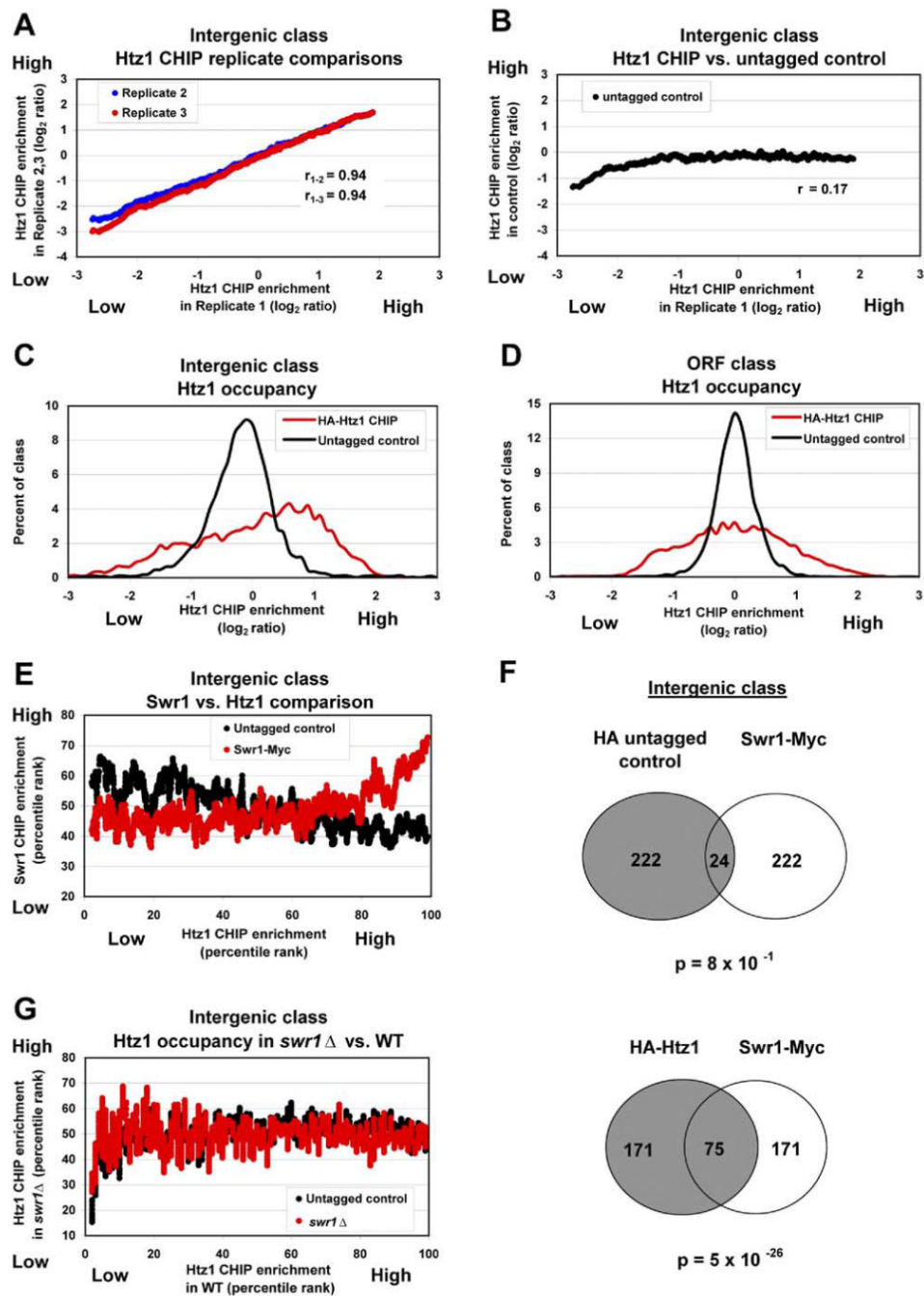
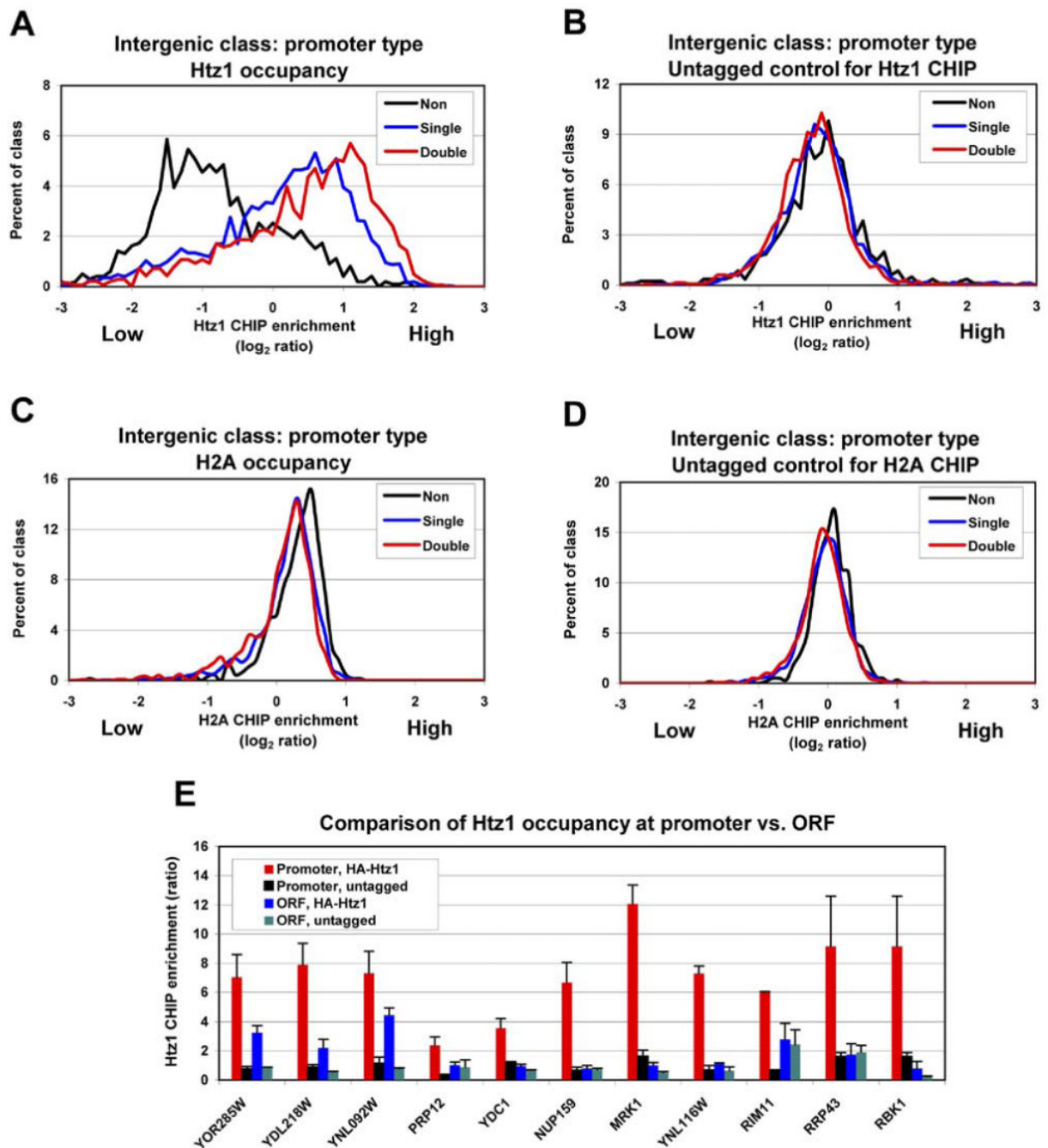


Figure 1.
Genome-Wide Localization of Htz1 and SWR1
(A) Htz1 occupancy is reproducible. Htz1 ChIP enrichment at IGRs from Replicate 1 (sorted by \log_2 ratio, x axis) versus Htz1 ChIP enrichment in Replicates 2 and 3, plotted as a moving average (window size 80, step 1) of the \log_2 ratios (y axis). ORF replicates yielded similar results (not shown). Strain: YBC1867.
(B) Htz1 occupancy is specific. Plotted as in (A), versus the untagged control (YBC1895).
(C and D) Htz1 ChIP is efficient. Distribution of the \log_2 median ratios of Htz1 ChIP enrichment at IGRs (C) or ORFs (D).
(E) Swr1 occupancy is efficient. Distribution of the \log_2 median ratios of Swr1 ChIP enrichment at IGRs (E) or ORFs (F).
(G) Htz1 occupancy is efficient in *swr1* Δ . Distribution of the \log_2 median ratios of Htz1 ChIP enrichment at IGRs (G) or ORFs (H) in *swr1* Δ versus WT.
(H) Htz1 occupancy is efficient in *swr1* Δ . Distribution of the \log_2 median ratios of Htz1 ChIP enrichment at IGRs (H) or ORFs (I) in *swr1* Δ versus WT.

(E) Htz1 occupancy is correlated with Swr1 occupancy. Htz1 ChIP enrichment at IGRs (sorted by percentile rank, x axis) versus Swr1 ChIP enrichment (YBC2170, or the untagged control strain YBC1895), plotted as the moving average (window size 40, step 1) of the percentile ranks (y axis).

(F) Venn diagrams depicting the overlap of IGRs with high levels of Htz1 and Swr1. The full dataset consisted of IGRs available in all three (Htz1, Swr1, and control) individual datasets (2457 IGRs total), from which we compared the top 10% of each.

(G) Swr1 is required for specific Htz1 deposition genome-wide. Htz1 ChIP enrichment in wt cells (sorted by percentile rank, x axis) versus Htz1 occupancy in *swr1* Δ mutants (YBC2162), plotted as the moving average (window size 40, step 1) of the percentile ranks (y axis).

**Figure 2.****Htz1 Prefers Promoters**

(A and B) Htz1 strongly prefers promoters genome-wide.

(C and D) H2A weakly prefers nonpromoters. IGRs were assigned to one of three promoter-type classes (see text). Htz1 or H2A occupancy in tagged (A and C) or untagged control strains (B and D). Htz1 enrichment (log₂ median ratio, x axis) versus the percent of IGRs in each promoter class (y axis). Strains for H2A ChIP: YBC2200 and YBC1894.

(E) Htz1 prefers promoters at individual genes. ChIP enrichment was determined by qPCR (note: *RRP43* and *RBK1* are divergent). Values are the average of three independent ChIPs with qPCR determination performed twice. Error bars: SD. The primer sets used for each

amplicon are listed in Table S2; format, (GeneID: promoter, ORF): *YOR285W*: D, F; *YDL218W*: I, K; *YNL092W*: O, Q; *PRP12*: U, V; *YDC1*: Y, AA; *NUP159*: AC, AE; *MRK1*: AF, AG; *YNL116W*: AH, AI; *RIM11*: AJ, AK; *RRP43*: AM, AL; *RBK1*: AM, AN. Values are normalized to an amplicon within *iYMR325W*, using primer set A.

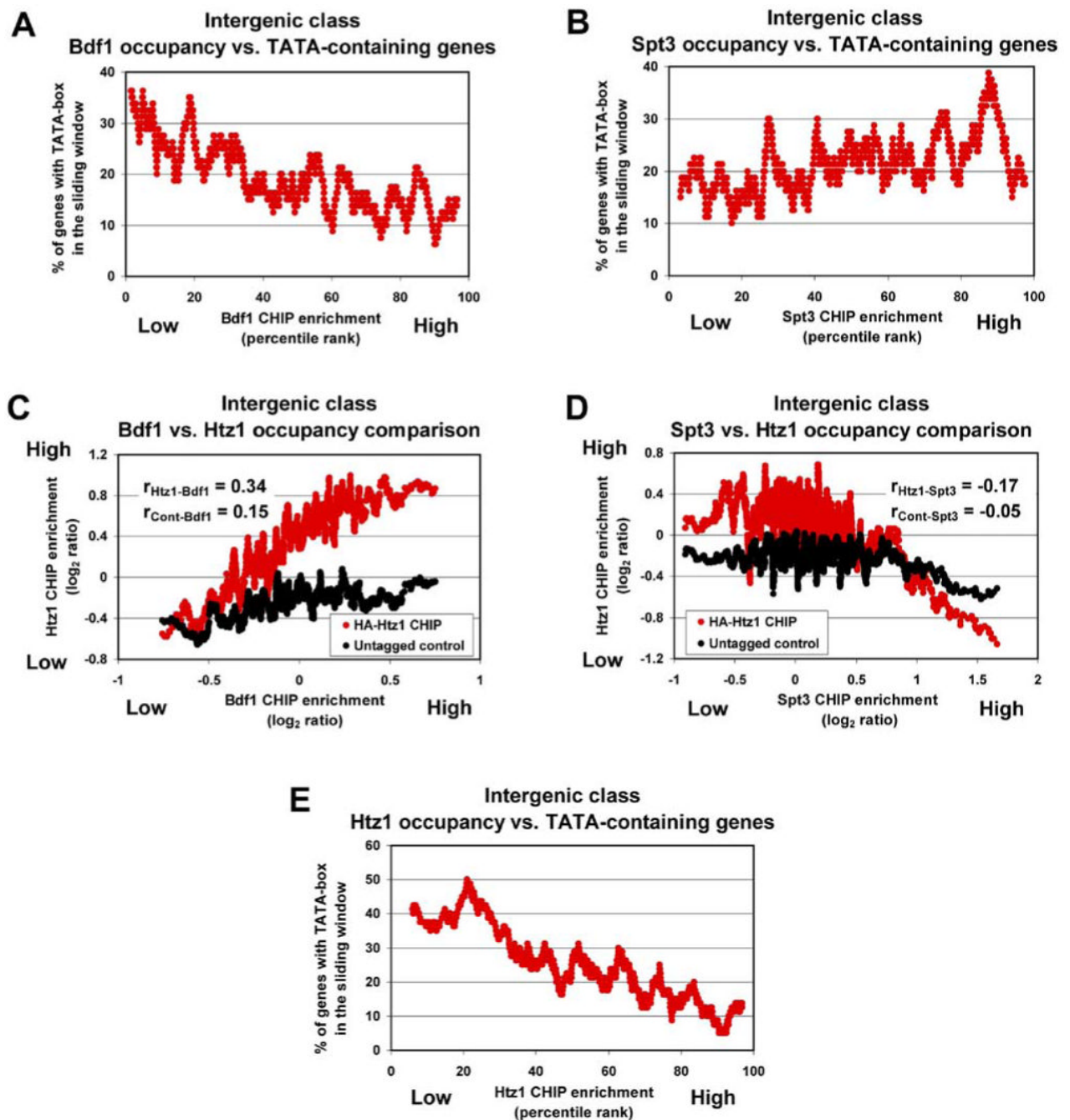


Figure 3.

Htz1 Occupancy Is Correlated with Bdf1 and Shows a Preference for TATA-less Promoters

(A) Bdf1 prefers TATA-less promoters.

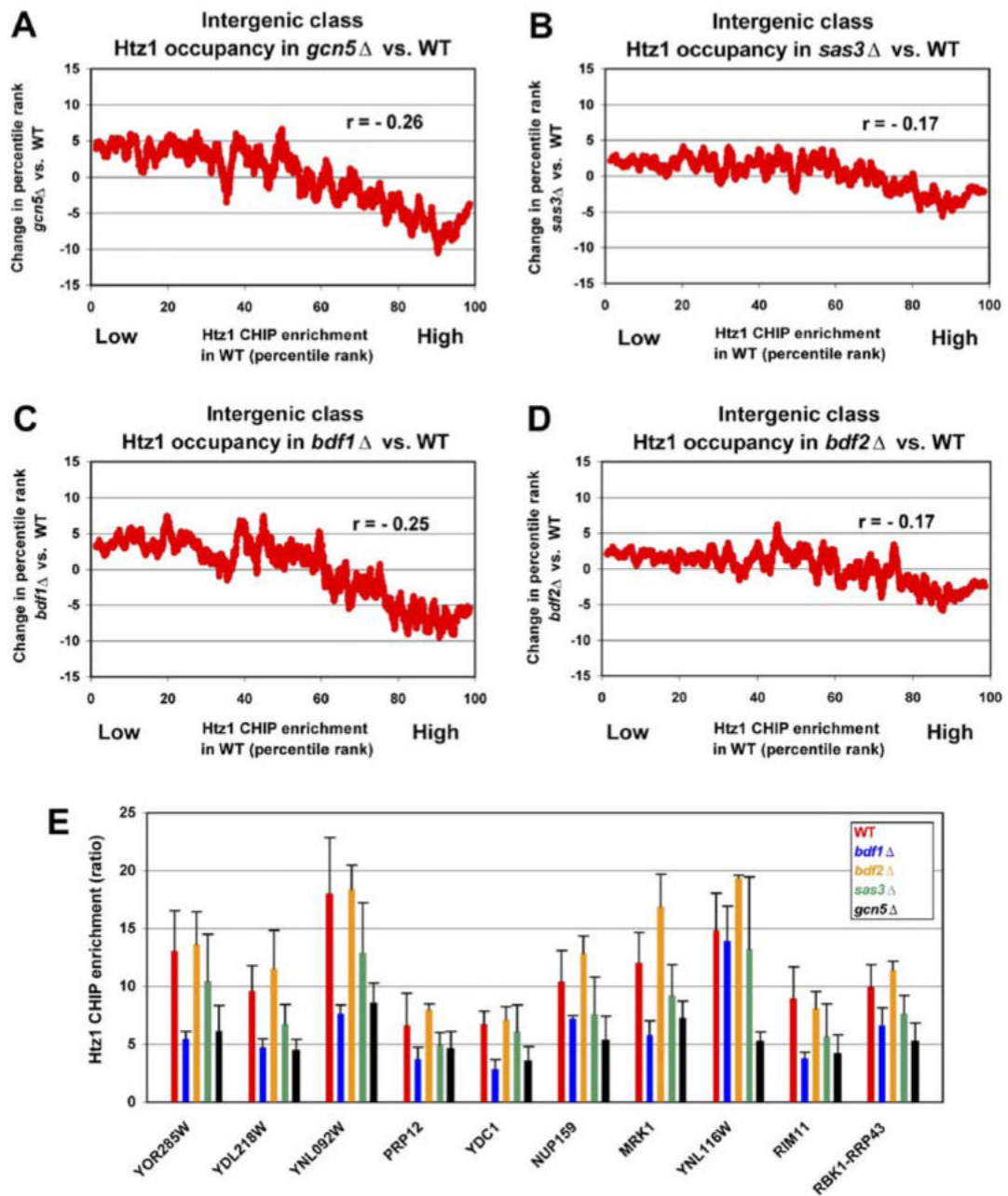
(B) Spt3 weakly prefers TATA-containing promoters.

(C) Occupancy correlation between Htz1 and Bdf1. Bdf1 occupancy at IGRs (sorted by \log_2 ratio, x axis) versus Htz1 occupancy, plotted as the moving average (window size 40, step 1) of the \log_2 ratio (y axis).

(D) Occupancy correlation between Htz1 and Spt3. As in (C), IGRs were sorted by \log_2 ratio of Spt3 ChIP (x axis).

(E) Htz1 prefers TATA-less promoters.

Plots for (A), (B) and (E): factor occupancy (single promoter class, sorted by percentile rank, x axis) compared to the fraction of promoters containing a TATA element (in a sliding window of 80 genes, as a percent of total, y axis). Bdf1 occupancy data is from Kurdistani et al. (2004), and Spt3 occupancy data is from Zanton and Pugh (2004).

**Figure 4.**

Strains Lacking Gcn5 or Bdf1 Display Reductions in Htz1 Occupancy

(A-D) Htz1 occupancy at IGRs in wt cells (sorted by percentile rank, x axis) was compared to Htz1 occupancy in mutant strains. Changes in Htz1 occupancy (Δ MPR; MPR in mutant - MPR in wt) in mutants were plotted as a moving average of 80 genes (window size 80, step 1, y axis).

(E) Relative abundance of Htz1 at 10 promoters in wt (YBC1894), *gcn5*Δ (YBC1662), *sas3*Δ (YBC1911), *bdf1*Δ (YBC2512), and *bdf2*Δ (YBC2513). ChIPs utilized polyclonal α Htz1 antibody, and values are the average of three independent ChIPs quantified by qPCR. Error bars: SD. Primer sets as in Figure 2 (Z, for *YDC1*).

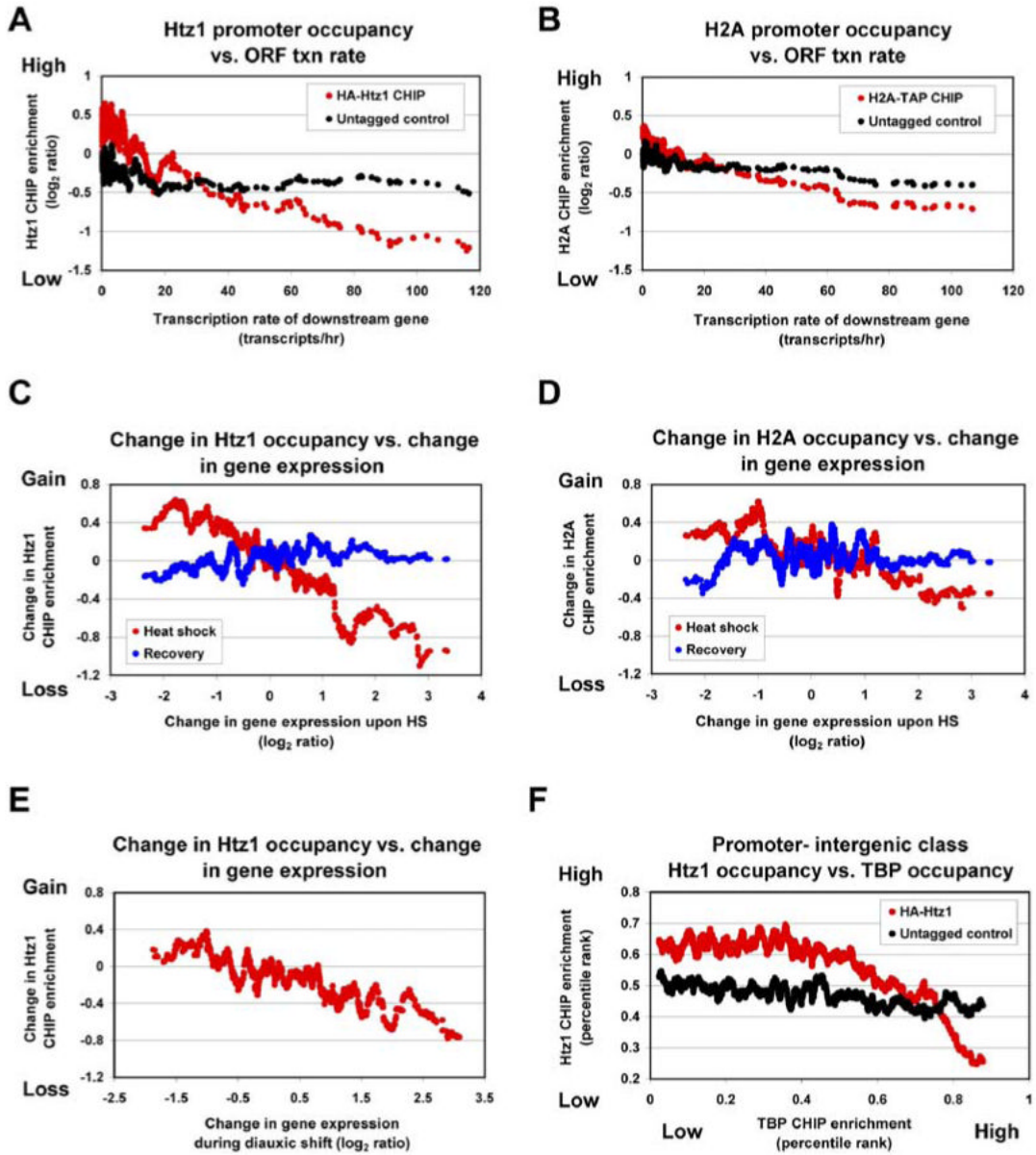
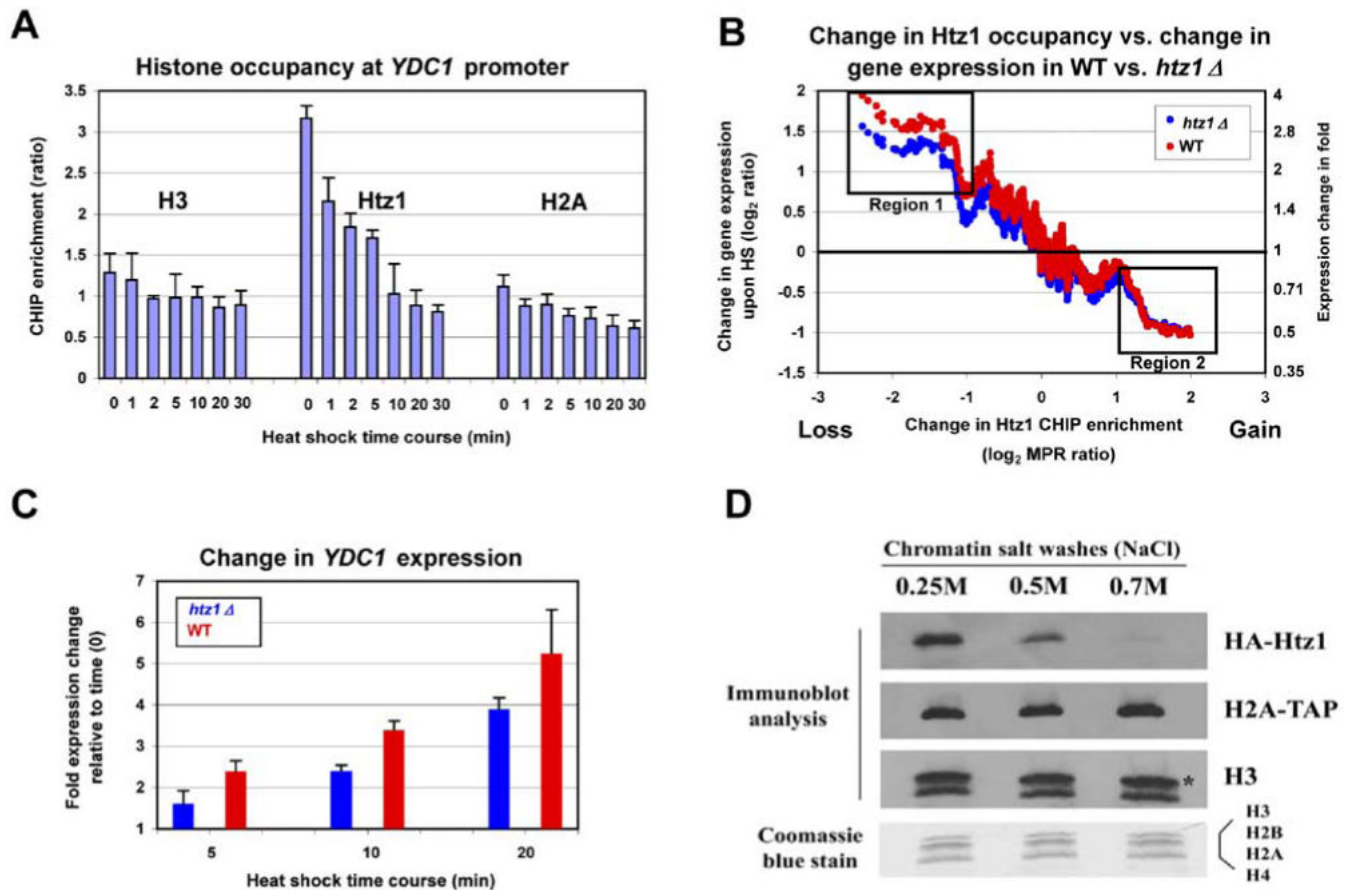


Figure 5. Htz1 Is Negatively Correlated with Transcription and Redistributes as Transcription Changes (A and B) Htz1 is negatively correlated with transcription and to a greater extent than H2A. Genes were sorted by transcription rate (x axis), and compared to Htz1 occupancy (A) or H2A occupancy (B), plotted as the moving average (window size 40, step 1) of ChIP enrichment (log₂ ratio, y axis). (C) During HS, Htz1 abandons activated promoters and occupies repressed promoters. Changes in gene expression resulting from HS (30 min) were quantified by microarray analysis and sorted according to their magnitude (log₂ ratios, x axis). Values are the average of three biological replicates. Htz1 occupancy during HS (30 min) or following recovery from HS (30 min after their return to 25°C). Plots depict the moving average (window size 40, step 1) of the change in Htz1 ChIP enrichment relative to time zero (no HS), either during HS or following the recovery from HS (y axis: log₂ [MPR ratio (HS or recovery/no HS)]). (D and E) Plot parameters as in (C).

- (D) H2A occupancy decreases slightly at activated promoters in response to HS.
- (E) Htz1 dynamics during diauxic shift. Conditions: 8hr growth to a final OD₆₀₀ of 6.2. Values are the average of two biological replicates.
- (F) Htz1 and TBP occupancy are negatively correlated. TBP occupancy (promoter IGRs, Pol III targets omitted) was sorted (by percentile rank, x axis) and plotted against a moving average (window size 80, step 1) of Htz1 occupancy (percentile rank, y axis).

**Figure 6.**

Htz1 Is Susceptible to Loss, Which Both Accompanies and Facilitates Activation

(A) During activation of *YDC1*, Htz1 is lost to a greater extent than H2A or H3. Histone ChIP enrichment at *YDC1* promoter was determined by qPCR (primer set Y). Values are the average of three independent ChIPs with qPCR determination performed twice. Error bars: SD. Strains: YBC2128 (Htz1 and H3 ChIPs) and YBC2228 (H2A ChIPs).

(B) Deletion of *HTZ1* attenuates activation but not repression in response to HS. The change in Htz1 occupancy in wt upon HS (30 min; sorted by \log_2 [MPR ratio (HS/no HS)], x axis) at each promoter was compared to the change in the expression of their linked ORFs in wt and *htz1* Δ strains, plotted as the moving average (window size 40, step 1) of expression changes upon HS (y axis). Boxes denote regions of the graph discussed in the text.

(C) *HTZ1* is required for full activation of *YDC1* in response to HS. Changes in *YDC1* expression during HS time course in wt, and *htz1* Δ strains were quantified by microarray analysis, and values are the average of three biological replicates. Error bars: SD.

(D) Htz1 is more susceptible to loss from yeast chromatin than is H2A or H3. Chromatin was prepared from a strain (YBC2228) bearing HA-Htz1 and H2A-TAP alleles. Equal portions were treated with increasing levels of sodium chloride (indicated), supernatants were removed, and the resulting chromatin pellet was treated with MNase to generate mononucleosomes. Histones were separated by SDS-PAGE and immunoblotted (anti-HA, anti-Protein A, and polyclonal α H3 antibodies were used, respectively), or stained with Coomassie blue dye (bottom panel). Asterisk denotes full-length H3 and the lower band a common proteolytic product.

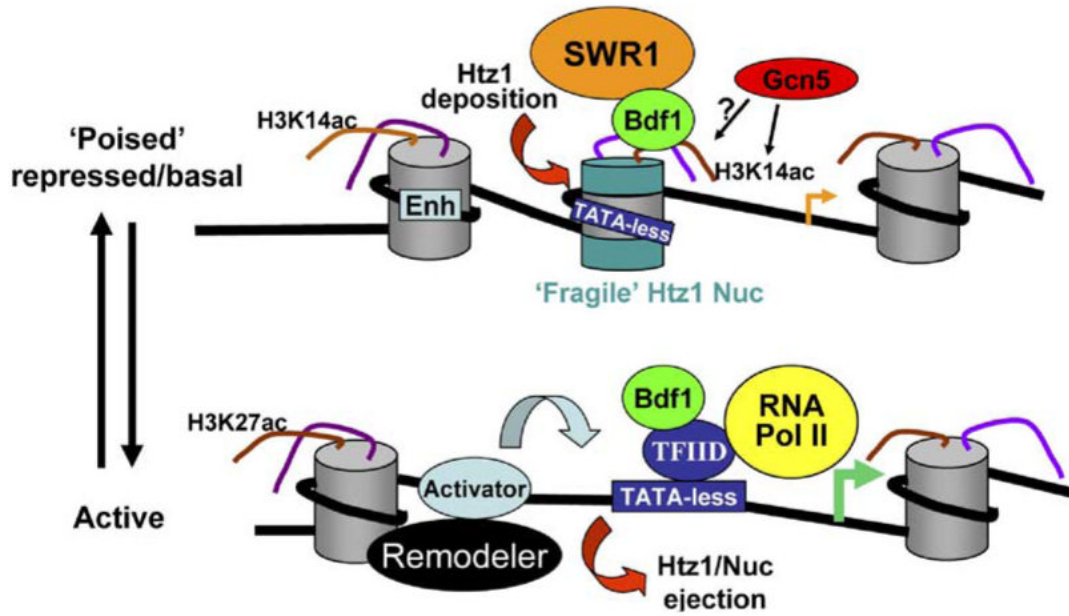


Figure 7.

A Model for Htz1 in Transcriptional Regulation

An Htz1-containing nucleosome (green disks, central nucleosome) occupies the promoters of certain repressed/basal genes, with a preference for TATA-less promoters. The deposition process requires SWR1 complex and is facilitated/targeted by Bdf1 and the acetyltransferase Gcn5. Acetylation of H3K14 and other residues by Gcn5 (and other HATs) likely underlies the observed correlations between histone acetylation and Htz1 occupancy. Although present during repression, Htz1 does not have a specialized function that promotes repression. Rather, biochemical experiments and occupancy dynamics establish the Htz1 nucleosome as susceptible to ejection (“fragile”), suggesting that the presence of Htz1 poises the repressed and basal states for full activation. Transition to the active state typically involves the action of chromatin remodeling factors (black oval) and the binding of activators to the enhancer (Enh). These factors likely collaborate to eject the Htz1 nucleosome, which facilitates activation by exposing promoter DNA to TFIIID and other transcription factors.

Table 1

Correlation (r) of Htz1 Occupancy with Histone Acetylation

Lysines	r	p Value
H2AK7ac	0.22	$<1.00 \times 10^{-16}$
H2BK11ac	0.12	1.15×10^{-5}
H2BK16ac	0.15	2.98×10^{-8}
H3K9ac	-0.26	$<1.00 \times 10^{-16}$
H3K14ac	0.28	$<1.00 \times 10^{-16}$
H3K18ac	-0.20	2.21×10^{-13}
H3K23ac	0.06	2.27×10^{-2}
H3K27ac	-0.35	$<1.00 \times 10^{-16}$
H4K8ac	0.21	1.45×10^{-14}
H4K12ac	0.11	6.98×10^{-5}
H4K16ac	-0.10	2.21×10^{-4}

Variance normalization data.